

# Lévy walks with velocity fluctuations

S. Denisov,<sup>1</sup> V. Zaburdaev,<sup>2</sup> and P. Hänggi<sup>1</sup>

<sup>1</sup>*Institute of Physics, University of Augsburg, Universitätsstrasse 1, D-86159 Augsburg, Germany*

<sup>2</sup>*School of Engineering and Applied Sciences, Harvard University, 29 Oxford street, Cambridge, MA 02138, USA*

(Dated: February 19, 2022)

The standard Lévy walk is performed by a particle that moves ballistically between randomly occurring collisions, when the intercollision time is a random variable governed by a power-law distribution. During instantaneous collision events the particle randomly changes the direction of motion but maintains the same constant speed. We generalize the standard model to incorporate velocity fluctuations into the process. Two types of models are considered, namely, (i) with a walker changing the direction and absolute value of its velocity during collisions only, and (ii) with a walker whose velocity continuously fluctuates. We present full analytic evaluation of both models and emphasize the importance of initial conditions. We show that the type of the underlying Lévy walk process can be identified by looking at the ballistic regions of the diffusion profiles. Our analytical results are corroborated by numerical simulations.

PACS numbers: 05.40.Fb, 05.45.Jn, 45.50.Jf

## I. INTRODUCTION

The concept of random walk is one of the cornerstones of statistical physics [1, 2]. It is a universal toolbox that can be used to study the dynamics of almost any physical system. Namely, the time evolution of the system can be represented by a trajectory,  $\mathbf{r}(t)$ , in the corresponding coordinate or state space. Then, the system dynamics can be quantified by a mean square displacement (MSD),  $\sigma(t) = \langle \mathbf{r}^2(t) \rangle$ . Whereas in the case of the standard Brownian dynamics the corresponding MSD scales linearly in time,  $\sigma(t) \sim t$ , the hallmark of many complex systems, *anomalous diffusion*, is characterized by a nonlinear time dependence of the MSD,  $\sigma(t) \sim t^\alpha$ , with  $\alpha \neq 1$  [3].

The phenomenon of anomalous diffusion is pertinent to the processes whose dynamics is dominated by long time or/and space correlations [4]. The case of superdiffusion,  $\alpha > 1$ , constitutes an intriguing limit. Real-life superdiffusive dynamics implies that a walker – an atom in an optical lattice [5], a tracer in a turbulent flow [6], a predator hunting for food [7], or a mussel in a bunch of peers [8] – explores its environment much faster than its Brownian ‘colleagues’ while still moving with a bounded velocity,  $|\mathbf{v}| < v_{\max}$ . The corresponding space-time dynamics is constrained to a cone, so that at a given time  $t$  the walker is always located within the space region  $|\mathbf{r}(t) - \mathbf{r}(0)| \leq v_{\max}t$ .

The Lévy-walk (LW) process [9] represents a simplest stochastic model which combines both key ingredients, that are the superdiffuse evolution and the finiteness of the velocity of motion. In one-dimensional case the standard LW process can be sketched as follows: a walker performs a sequence of mutually uncorrelated ballistic flights of random duration but of fixed velocity,  $v_0$ . The flights are separated by the instantaneous collisions at which the walker changes the direction of its motion, taking randomly either negative or positive direction. The time between consecutive collisions, and, therefore, the duration of a single-flight event, is distributed according

to a probability density function (PDF),  $\psi(\tau)$ , with a power-law asymptotic

$$\psi(\tau) \propto (\tau/\tau_0)^{-\gamma-1}, \quad (1)$$

where a constant  $\tau_0$  sets the characteristic timescale. The exponent  $\gamma$  in Eq.(1) determines explicitly the scaling of the corresponding MSD. Namely,  $\alpha = 1$  when  $\gamma > 2$  (normal diffusion),  $\alpha = 3 - \gamma$  when  $1 < \gamma < 2$  (superdiffusion), and the choice of the exponent from the interval  $0 < \gamma < 1$  leads to the ballistic diffusion,  $\alpha = 2$  [9]. If an ensemble of particles, initially localized at  $x = 0$ , starts to spread at time  $t = 0$ , the corresponding propagators, i. e. the PDFs to find a particle at a point  $x$  at a time  $t$ , are all restricted to the cone  $[-v_0t, v_0t]$ , but have different shapes – Gaussian profiles in the case of normal diffusion, profiles in a form of Lévy distributions in the case of superdiffusion, and U-shaped profiles in the ballistic limit [10]. Note, however, that all three propagators exhibit a sharp cutoff at the points  $|x| = v_0t$ .

In addition to the examples already listed, the LW formalism has found other successful applications, such as the description of DNA nucleotide patterns [11], modeling the dynamics of an ion placed into an optical lattice [12], analysis of the evolution of magnetic holes in ferrofluids [13], and engineering of Lévy glasses [14]. The LW ideology is flexible and leaves room for potential generalizations and modifications thus allowing to construct and tailor models which are able to mimic real processes in greater detail. For example, the condition of the constant velocity of ballistic motion is barely the case in real systems – neither a foraging deer [15] nor an ion moving through the optical lattice [12] are subjected to this strict condition. It is therefore worthwhile to construct extensions of the standard LW model that are able to take into account the effects of velocity fluctuations.

Although it is intuitive that the light-cone cutoff will be smeared by velocity variations, no further insight can be achieved without specification of the statistical properties of velocity fluctuations and their generating mechanisms.

In this paper, we develop two generalizations of the standard one-dimensional LW scheme which include velocity alternations. For the same flight-time PDF, Eq.(1), both models yield the same MSD exponent and produce identical profiles of propagators in the *innermost region* of the propagation cone. Of special importance are the *ballistic regions*, where the shape of propagators exhibits a model-specific behavior.

The paper is structured as follows. In Sec. II we define the models. In Sec. III we construct the corresponding transport equation for propagators and discuss the role of initial conditions. Section IV is devoted to the asymptotic analysis of propagator profiles, especially at the regions of ballistic fronts. Section VI summarizes the results of the paper and discusses possible applications of the proposed formalism.

## II. MODELS

### A. Model A: Lévy walk with alternating velocities

Consider a LW process where a particle performs every ballistic flight with constant speed but randomly changes it during scattering events between the flights. Velocity  $v$  is now a random variable governed by a certain PDF,  $h(v)$ . A trivial bimodal PDF of a form

$$h(v) = [\delta(v - v_0) + \delta(v + v_0)]/2 \quad (2)$$

corresponds to the standard LW scheme [9]. Velocity dynamics introduces an additional degree of freedom to the process, so that the resulting type of diffusion is determined now both by the flight-time PDF,  $\psi(\tau)$ , see Eq.(1), and the velocity distribution,  $h(v)$ . Here we consider a particular case when the delta-function in Eq.(2) is replaced by a hump-like distribution of finite variance,  $\delta(v) \rightarrow \Delta(v)$ ,  $\Sigma_A^2 = \int_{-\infty}^{\infty} v^2 \Delta(v) dv < \infty$ . Since this work deals with *velocity fluctuations*, below we will assume that the variance of humps is small compared to the average speed,  $\Sigma_A \ll v_0$ .

### B. Model B: Lévy walk with fluctuating velocity

Consider a random walk process, where the velocity of a walker is not constant during the single flight event but fluctuates around an average value,  $v_0$ . Phenomenologically, these fluctuations can be attributed either to some internal mechanisms – chaotic precession of the magnetic moment of a ferrofluid particle that modifies the interaction of the particle with an external magnetic field [16],

or complex neural processes in the brain of foraging bumblebee [15], or to some external mechanisms, like interaction of a moving nano-colloidal particle with an active medium [17]. A particular variant of this model has been introduced in Ref. [18], where it has been used to describe the perturbation spreading in one-dimensional many-particle systems.

The dynamics of the particle during a single flight event can be described by a Langevin equation,

$$\dot{x} = v_0 + \xi(t), \quad (3)$$

where  $\xi(t)$  is a Gaussian delta-correlated noise with zero-mean and finite variance,  $\langle \xi(t), \xi(t') \rangle = D_v \delta(t - t')$ ,  $D_v > 0$ . By integrating the above equation over some interval of time  $\tau$ , we obtain:

$$x(t + \tau) = x(t) + v_0 \tau + w(\tau) \quad (4)$$

The new stochastic variable,  $w(\tau) = \int_t^{t+\tau} \xi(t') dt'$ , can be characterized by a PDF  $p(w, \tau)$ , which is a Gaussian distribution with a dispersion  $\Sigma_B^2 = \langle (x - v_0 t)^2 \rangle = D_v \tau$ . Therefore, if a particle starts its flight of duration  $\tau$  at a point  $x$  with a velocity  $v_0$ , it will arrive at the point  $x + v_0 \tau + w(\tau)$ , where  $w$  is a random variable with the PDF  $p(w, \tau)$ .

Having the microscopic descriptions of both models, we can now derive the evolution equations for the corresponding propagators,  $P(x, t)$ .

## III. EVOLUTION EQUATIONS FOR PROPAGATORS

We start with derivation of an evolution equation for the propagator of a combined model,  $A \otimes B$ . The corresponding process is generated by a walker that chooses its velocity from a distribution  $h(v)$  at the beginning of the  $i$ -th flight,  $v_i$ , and then moves unidirectionally, with the instantaneous velocity,  $\tilde{v}_i(t)$ , fluctuating around  $v_i$ . The velocity fluctuations are characterized by an universal PDF,  $p(w, t)$ . Transport equations for a model,  $A$  or  $B$ , can be obtained as particular cases either by setting  $D_v = 0$  (model  $A$ ) or assuming  $h(v) = [\delta(v - v_0) + \delta(v + v_0)]/2$  (model  $B$ ).

We follow the standard procedure [19, 20], and introduce a space-time PDF for the collision events,  $\nu(x, t)$ , which gives the probability to observe collision in a point  $x$  at a time  $t$ . It satisfies the following balance equation:

$$\nu(x, t) = \int_{-\infty}^{\infty} \int_{-\infty}^{\infty} dv dw \int_0^t \nu(x - v\tau - w, t - \tau) \psi(\tau) h(v) p(w, \tau) d\tau + \varphi(t) \int_{-\infty}^{\infty} h(v) p(x - vt, t) dv. \quad (5)$$

Here we assumed that all particles were launched from the point  $x = 0$ , i.e.  $P(x, t = 0) = \delta(x)$ . The first summand on the right hand side of Eq.(5) accounts for the particles that had changed the direction of their flights before the observation time  $t$ , while the second term accounts for the particles that were flying during the whole observation time. If a particle starts at  $x = 0$  with a certain velocity  $v$ , the position of the first scattering event is influenced by the velocity fluctuations and is given by

---


$$P(x, t) = \int_{-\infty}^{\infty} \int_{-\infty}^{\infty} dv dw \int_0^t \nu(x - v\tau - w, t - \tau) \Psi(\tau) h(v) p(w, \tau) d\tau + \Phi(t) \int_{-\infty}^{\infty} h(v) p(x - vt, t) dv. \quad (6)$$

Here  $\Psi(t)$  is the probability to continue the flight that started at  $\tau = 0$  up to time  $t$ ,

$$\Psi(t) = 1 - \int_0^t \psi(\tau) d\tau. \quad (7)$$

The second summand on the right hand side of Eq.(6) is weighted with the function  $\Phi(t)$ , which is the probability to continue the very first flight during the whole observation time  $t$ . Both functions,  $\varphi(t)$  and  $\Phi(t)$ , explicitly depend on the type of initial conditions that we are going to discuss in the following subsection.

### A. Equilibrated vs. non-equilibrated initial conditions

There are two types of initial conditions which are relevant in the physical context [21].

The first type, the so-called *non-equilibrated* initial condition, assumes that all particles started their first flights at  $t = 0$ . In this case we have

$$\varphi(t) \equiv \psi(t), \quad (8)$$

$$\Phi(t) \equiv \Psi(t). \quad (9)$$

The second type, the *equilibrated* initial conditions, corresponds to the situation when all particles are already in the stationary regime at time  $t = 0$ . That means that every particle was initially in the state of flight with probability one, and all of them have long (possibly infinite) 'walking' histories. The following thought experiment might help to understand the equilibrated setup better. Assume that an ensemble of particles was created at  $t = -t_1$ . At the time  $t = 0$  we take the actual position of every particle as a reference point, from which we count the displacement of the particle for time  $t > 0$ . It may be considered as though at initial time  $t = 0$  we instantaneously tagged all particles to the point  $x = 0$ , without affecting their performance. The limit  $t_1 \rightarrow \infty$  corresponds to the equilibrated setup.

the PDF  $\int_{-\infty}^{\infty} \delta(x - vt - w) p(w, t) dw = p(x - vt, t)$ . The prefactor of the second integral in Eq.(5),  $\varphi(t)$ , defines the PDF of having the first scattering event at time  $t$ . We shall specify the exact functional form of  $\varphi(t)$  in the next subsection, when addressing two different types of initial conditions.

The PDF  $\nu(x, t)$  allows us to define the corresponding propagator,

---

Consider now Eq.(5) for  $P(x, t = 0) = \delta(x)$  without velocity fluctuations and in the non-equilibrated setup, meaning that  $\varphi(t) = \psi(t)$ . This so simplified integral equation can be solved by applying the Laplace transform with respect to time  $t$ . Convolution integrals are rendered as algebraic products in the Laplace space and, therefore, the frequency of velocity changes is given by the following expression,

$$\overline{\nu}(s) = \frac{P_0 \overline{\psi}(s)}{1 - \overline{\psi}(s)}. \quad (10)$$

Here, an overline denotes the Laplace transform and  $s$  is the coordinate in the Laplace space. In general, the PDF for a particle to experience a collision after the start of observation depends on how long a timespan this particle was flying before. Therefore, for any particle at a time  $t$ , we like to know its flight time. The corresponding PDF,  $N(t, \tau)$ , shows how many particles at the given point in time have a flight time  $\tau$ :

$$N(t, \tau) = \Psi(\tau) \nu(t - \tau) + \Psi(\tau) \delta(t - \tau). \quad (11)$$

Again, with the help of the Laplace transform and using its shift property we find:

$$\overline{N}(\tau, s) = \frac{\Psi(\tau) e^{-s\tau}}{1 - \overline{\psi}(s)}. \quad (12)$$

Consider now the limit of large times, that in the Laplace space corresponds to small values of  $s$ . If the mean flight time exists, i.e.,  $\langle \tau \rangle = \int_0^{\infty} \tau \psi(\tau) d\tau < \infty$ , which is always the case for  $\gamma > 1$ , the leading terms in the expansion of the Laplace transform  $\overline{\psi}(s)$  with respect to small  $s$  can be written as  $\overline{\psi}(s) \simeq 1 - s \langle \tau \rangle$ . Substituting it into Eq. (12) and inverting the Laplace transform we arrive at

$$N(t, \tau) = \frac{\Psi(\tau)}{\langle \tau \rangle}. \quad (13)$$

This is yet another way to arrive at the central result of the renewal theorem [22], see also [21, 23, 24]. Now,

when we know the distribution of particles with respect to their flight times  $\tau$ , we can calculate the PDF of the first collision after the process has been initiated,  $\varphi(t)$ . By using the conditional probability formula we obtain:

$$\varphi(t) = \int_0^\infty \frac{N(\tau)\psi(t+\tau)}{\Psi(\tau)} d\tau \quad (14)$$

A similar expression can be written for the probability of having no collisions before time  $t$ ,  $\Phi(t)$ . Substituting the distribution over the flight times, Eq. (13), in the above equation we arrive at:

$$\varphi(t) = \langle \tau \rangle^{-1} \int_0^\infty \psi(t+\tau) d\tau, \quad (15)$$

$$\Phi(t) = \langle \tau \rangle^{-1} \int_0^\infty \Psi(t+\tau) d\tau. \quad (16)$$

Different types of initial conditions naturally correspond to different experimental setups. If an ensemble of random walkers has been created and then immediately launched, then the non-equilibrated initial conditions is the proper setting. However, if the ensemble has already been evolved for a while, before one starts to measure ensemble characteristics, the equilibrated initial conditions would be the appropriate choice.

As it can be seen from Eqs. (8, 9) and Eqs. (15, 16), the case of equilibrated initial conditions is characterized by a more pronounced influence of the initial distribution of particles on the propagator evolution. We will unfold this important observation in the subsequent section.

## B. Solution of the evolution equations

Equations (5-6) can be studied further by using the combined Fourier and Laplace transforms in space and time domains correspondingly. Taking into account the shift property of the integral transform and convolution form of the integrals, the original equations (5-6) can be reduced to the system of algebraic equations:

$$\begin{aligned} \tilde{\nu}(k, s) &= \tilde{\nu}(k, s) \left[ \overline{\widehat{h}(k\tau)\widehat{p}(k, \tau)\psi(\tau)} \right] + \left[ \overline{\widehat{h}(kt)\widehat{p}(k, t)\varphi(t)} \right] \\ \tilde{P}(k, s) &= \tilde{\nu}(k, s) \left[ \overline{\widehat{h}(k\tau)\widehat{p}(k, \tau)\Psi(\tau)} \right] + \left[ \overline{\widehat{h}(kt)\widehat{p}(k, t)\Phi(t)} \right] \end{aligned}$$

We used overline and hat notations to denote the Laplace and Fourier transforms, and the tilde notation for their combination, whereas  $k$  ( $s$ ) denote the coordinates in the corresponding Fourier (Laplace) space. The above system can be resolved straightforwardly, yielding,

$$\begin{aligned} \tilde{P}(k, s) &= \frac{\left[ \overline{\Psi(\tau)\widehat{h}(k\tau)\widehat{p}(k, \tau)} \right] \left[ \overline{\varphi(t)\widehat{h}(kt)\widehat{p}(k, t)} \right]}{1 - \left[ \overline{\widehat{h}(k\tau)\widehat{p}(k, \tau)\psi(\tau)} \right]} \\ &+ \frac{\left[ \overline{\widehat{h}(kt)\widehat{p}(k, t)\Phi(t)} \right]}{\left[ \overline{\widehat{h}(k\tau)\widehat{p}(k, \tau)\psi(\tau)} \right]}. \end{aligned} \quad (17)$$

Note that no prior assumptions concerning the velocity, flight time or noise PDF's were made before to obtain the *formal* solution in Eq. (17). An attribute 'formal', aside from denoting an exact character of the final result, also carries a certain negative tone. Namely, it is practically impossible to handle such a complex expression as Eq.(17), especially when trying to map it backward onto the original space-time domain. There are only two possibilities left, namely, either to resort to asymptotic analysis or to perform direct numerical calculations. We are going to pursue both options in the section below.

## IV. ASYMPTOTIC ANALYSIS

The parameter space of the general model, given by Eqs. (5, 6), is a highly-dimensional space and its detailed exploration is outside the scope of the present work. We remind that we are interested in the limit when velocity fluctuations are small compared to the characteristic velocity of walkers. For the model *A* that assumes the limit  $\Sigma_A \ll v_0$ , while for the model *B* it means that  $\sqrt{D_v} \ll v_0$ . It should be also noted that there are two types of contributions to the overall propagator. The first term on the right hand side of Eq.(6) describes the self-similar evolution of the particles that form the central part of the density profile, whereas the second term is a contribution which stems from the initial conditions and describes the behavior of the ballistic fronts. These contributions should be analyzed in more detail, and below we analyze them separately.

### A. Central part of the density distribution

The essence of the asymptotic analysis routinely employed in random walks is to look at the large time and space limit,  $x, t \rightarrow \infty$ , which corresponds to the limit of small values of  $k$  and  $s$  in the Fourier/Laplace space,  $k, s \rightarrow 0$  [2]. Therefore instead of using the full expressions for the corresponding transforms, only the leading terms in their expansions with respect to small  $k$  and  $s$  should be retained. It is possible to show that at the limit of small velocity fluctuations the asymptotic behavior of the central part of the propagators for both models is identical to that of the standard Lévy walk process [9]. In the case of Lévy walks, when  $p(w, t) = \delta(w)$ , the first term on the right hand side of the general expression given in Eq. (17) can be rewritten as:

$$\tilde{P}^{\text{LW}} = \frac{[\overline{\Psi(s+ikv_0)+\Psi(s-ikv_0)}][\overline{\varphi(s+ikv_0)+\varphi(s-ikv_0)}]}{2 - [\overline{\psi(s+ikv_0)+\psi(s-ikv_0)}]} \quad (18)$$



For the analysis of its asymptotic properties we make use of the expansion:

$$\begin{aligned} \overline{\psi}(s \pm ikv_0) &\simeq 1 - \frac{\tau_0}{\gamma - 1}(s \pm ikv_0) - \Gamma[1 - \gamma]t_0^\gamma(s \pm ikv_0)^\gamma \\ &+ \frac{\tau_0^2}{(\gamma - 2)(\gamma - 1)}(s \pm ikv_0)^2 + O((s \pm ikv)^{1+\gamma}). \end{aligned} \quad (19)$$

Depending on  $\gamma$  certain terms in the above expression take the leading role thus defining three major scaling regimes [10]. For  $\gamma > 2$  the mean square of the flight distance,  $\langle (v_0\tau)^2 \rangle$ , is finite, so that the corresponding transport process is the normal diffusion. In the intermediate regime,  $1 < \gamma < 2$ , the mean squared flight distance diverges. In this regime the leading term of  $k$  scales like  $k^\gamma$  thus leading to anomalous diffusion and Lévy-like profiles of the corresponding propagators. Finally, long flights dominate the process at the limit  $0 < \gamma < 1$ , thus forming U-shaped propagators [9].

In the case of anomalous superdiffusion,  $1 < \gamma < 2$ , the Laplace/Fourier image of the propagators of both models, *A* and *B*, in the limit of small  $k$  and  $s$ , is given by:

$$\tilde{P}^{\text{LW}} \simeq \frac{1}{s + \tau_0^{\gamma-1} v_0^\gamma (\gamma - 1) \Gamma[1 - \gamma] k^\gamma \sin(\pi\gamma/2)}. \quad (20)$$

In the space-time domain it corresponds to the Lévy distribution with a characteristic power-law behavior of tails, exhibiting the following scaling properties [9, 10]:

$$P(x, t') \simeq \frac{1}{K u^{1/\gamma}} P\left(\frac{x}{K u^{1/\gamma}}, t\right), \quad |x| \ll v_0 t, \quad (21)$$

where  $K \propto \tau_0^{1-1/\gamma} v_0$  and  $u = t'/t$ .

Therefore, in the limit of small velocity fluctuations and for  $1 < \gamma < 2$ , the central part of the PDF is universal and is given by the well-known Lévy walk propagator [9].

## B. Ballistic humps

The ballistic regions are model specific. Therefore, their analysis on the base of the combined model, introduced in Sec. III, is impossible and two models should be considered separately.

Relations (5-6) tell us that ballistic humps are formed by the particles which were flying from the very beginning, i.e., they either started their flight or they were already in the state of flying at the time  $t = 0$ . Therefore the expression for the PDF in the ballistic hump regions reads

$$P_{\text{hump}}(x, t) = \Phi(t) \int_{-\infty}^{\infty} h(v) p(x - vt, t) dv. \quad (22)$$

Now the difference between two models, *A* and *B*, is evident. In the case of random velocities, that is the case

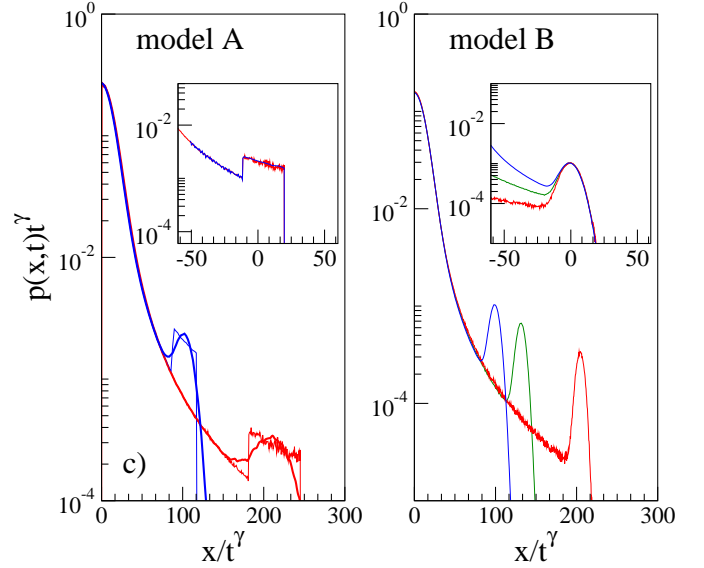


FIG. 1. (color online) Rescaled propagators for generalized Lévy-walk processes with the exponent  $\gamma = 5/3$ ; at times  $t = 100$  and  $600$  for model *A* (left panel), and at  $t = 100, 400$ , and  $600$  for model *B* (right panel) for equilibrated initial conditions. The profiles for the model *A* are shown for two different velocity probability distribution functions,  $\Delta(v)$ , rectangular and Gaussian, with the variance  $\Sigma_A^2 = 0.1$ . Other parameters are  $v_0 = 1$  and  $D_v = 0.1$ . The insets show the ballistic front regions as a function of a shifted coordinate,  $\bar{x} = x - v_0 t$ , with a width and height rescaled by the corresponding power laws listed in Table 1.

of model *A*, the width of the ballistic humps is proportional to the observation time  $t$  because the particles with slightly different initial velocities will separate ballistically, and the interparticle distances will grow linearly in time. The shape of a velocity PDF,  $h(v)$ , will be reproduced by the ballistic humps, see Fig. 1 (left panel). In the case of delta-like velocity distribution  $h(v)$ , see Eq. (2), but with velocity fluctuations, that is the case of model *B*, the particles flying from the very beginning will accumulate fluctuations during the spreading time, and, according to the central limit theorem, the width of the initially  $\delta$ -like ballistic peaks will grow as  $\sqrt{t}$ . The shape of the peaks will be always Gaussian.

The total number of particles in the hump, i.e., the area under the hump, is governed by the survival probability  $\Phi(t)$ . This number is the same for both models and depends on the type of the initial conditions. Already now we can say that the height of the humps decays faster for model *A*, since its width increases faster. By substituting the power-law flight time PDF, Eq.(1), into Eq. (22), we can explicitly calculate the scaling of the width, height, and total number of particles in the hump for two different models and two types of initial conditions. The result of the evaluation are presented with Table 1. For both models the equilibrated initial conditions lead to a slower decay of the hump height. On Fig. 1 we plot the propagators of both models for different

times, where for the model  $A$  we used two velocity PDFs,  $h(v)$ , with a Gaussian (thick solid lines) and a rectangular humps (thin lines) around characteristic velocity values  $\pm v_0$ , with  $v_0 = 1$ . Remarkably, the rectangular shape of the velocity PDF is directly translated into the shape of ballistic fronts. In the case of Gaussian PDF, ballistic humps look similar for both models. However, the time evolution reveals the dramatic difference in the scalings of the humps' profiles, see Fig.1 and Table 1.

TABLE I. Scaling properties of ballistic humps of three different random walk models, standard Lévy-walk (LW), process with alternating ( $A$ ) and fluctuating ( $B$ ) velocities, for equilibrated (eq.) and non-equilibrated (non-eq.) initial conditions. Here we address the regime of anomalous superdiffusion,  $1 < \gamma < 2$ .

Model	Initial condition	Scaling		
		width	height	area
LW	non-eq.	-	-	$t^{-\gamma}$
	eq.	-	-	$t^{1-\gamma}$
$A$	non-eq.	$t$	$t^{-1-\gamma}$	$t^{-\gamma}$
	eq.	$t$	$t^{-\gamma}$	$t^{1-\gamma}$
$B$	non-eq.	$t^{1/2}$	$t^{-1/2-\gamma}$	$t^{-\gamma}$
	eq.	$t^{1/2}$	$t^{1/2-\gamma}$	$t^{1-\gamma}$

## V. CONCLUSIONS.

In this paper we have presented two random walk models that describe stochastic transport phenomena with random velocities. Two different mechanisms of velocity fluctuations have been analyzed. These correspond to instantaneous alternations during collision events (model  $A$ ) and continuous velocity fluctuations during the flights (model  $B$ ). Both models can generate processes that exhibit anomalous superdiffusive behavior. However, corresponding diffusion profiles reveal essentially different behaviors in the ballistic regions, thus underlining the fact that ballistic fronts carry an important information about the origin of velocity fluctuations, maintaining memory of the initial conditions. Therefore, ballistic humps may serve as a diagnostic tool which allows to calibrate velocity fluctuations and explore the internal dynamics of a random walker. Our analytical results open the possibilities to study the evolution of complex systems, ranging from a bead moving in a colloidal medium to a motion of a bacterium, in which case velocity fluctuations are controlled by complex chemical circuits. Corresponding spatial-temporal patterns can be reproduced with relatively simple and transparent random walk models thus providing a new tool for the analysis of these patterns.

This work has been supported by the DFG Grant HA1517/31-2 (S.D. and P.H.) and DFG fellowship ZA593/2-1(V.Z.).

- 
- [1] G. H. Weiss, *Aspects and Applications of the Random Walk* (North-Holland, Amsterdam) 1994.
  - [2] J. Klafter and I. M. Sokolov, *First Steps in Random Walks* (Oxford University Press, Oxford) 2011.
  - [3] M. F. Shlesinger, G.M. Zaslavsky, and J. Klafter, *Nature* **363**, 31 (1993); J. Klafter, M. F. Shlesinger, and G. Zumofen, *Phys. Today* **49**(2), 33 (1996).
  - [4] P. Hanggi and F. Marchesoni, *Chaos* **15**, 026101 (2005).
  - [5] S. Marksteiner, K. Ellinger and P. Zoller, *Phys. Rev. A* **53**, 3409 (1996).
  - [6] T. H. Solomon, E. R. Weeks, and H. L. Swinney, *Phys. Rev. Lett.* **71**, 3975 (1993)
  - [7] G. M. Vismathan *et al.*, *Nature* **381**, 413 (1996); D. W. Sims *et al.*, *Nature* **451**, 1098 (2008); M. F. Shlesinger, *J. Phys. A: Math. Theor* **42**, 434001 (2009).
  - [8] M. de Jager *et al.*, *Science* **332**, 1551 (2011).
  - [9] M. F. Shlesinger and K. Klafter, *Phys. Rev. Lett.* **54**, 2551 (1985); M. F. Shlesinger, B. J. West, and J. Klafter, *Phys. Rev. Lett.* **58**, 1100 (1987); A. Blumen, G. Zumofen, and J. Klafter, *Phys. Rev. A* **40**, 3964 (1989).
  - [10] M. Schmiedeberg, V. Zaburdaev, and H. Stark, *J. Stat. Mech.* P12020 (2009).
  - [11] C. K. Peng *et al.*, *Nature* **356**, 168 (1992); S. V. Buldyrev *et al.*, *Phys. Rev. E* **47**, 4514 (1993).
  - [12] H. Katori, S. Schlipf, and H. Walther, *Phys. Rev. Lett.* **79**, 2221 (1997).
  - [13] S. Clausen, G. Helgesen, and A. T. Skjeltorp, *Phys. Rev. A* **58**, 4229 (1998).
  - [14] P. Barthélemy, J. Bertolotti, and D. S. Wiersma, *Nature* **453**, 495 (2008); J. Bertolotti *et al.*, *Adv. Funct. Mater.* **20**, 20 (2010).
  - [15] G. M. Viswanathan *et al.*, *Nature* **401**, 911 (1999).
  - [16] D. V. Berkov, N. L. Gorn, R. Schmitz, and D. Stock, *J. Phys.: Condens. Matter* **18**, S2595 (2006).
  - [17] A. Malevanets and R. Kapral, *J. Chem. Phys.* **112**, 7260 (2000).
  - [18] V. Zaburdaev, S. Denisov, and P. Hänggi, *Phys. Rev. Lett.* **106**, 180601 (2011).
  - [19] J. Klafter, A. Blumen and M.F. Shlesinger, *Phys. Rev. A* **35** 3081, (1987).
  - [20] V. Yu. Zaburdaev, M. Schmiedeberg, and H. Stark, *Phys. Rev. E* **79** 011119 (2008).
  - [21] J. K. E. Tunaley, *Phys. Rev. Lett.* **33** 1037 (1974).
  - [22] W. Feller, *An Introduction to Probability Theory, Vol. 2*, (Wiley, New York. 1971).
  - [23] J. W. Haus and K. W. Kerr, *Phys. Rep.* **150** 263 (1987).
  - [24] H. Scher and M. Lax, *Phys. Rev. B* **7**, 4491 (1973).